

Ultrafast spin dynamics in nickel

W. Hübner

Institut de Physique et Chimie des Matériaux de Strasbourg, Unite Mixte 380046, CNRS-ULP-EHICS, 23 rue du Loess, 67037 Strasbourg Cedex, France

and Max-Planck-Institut für Mikrostrukturphysik, Weinberg 2, D-06120 Halle, Germany

G. P. Zhang*

Max-Planck-Institut für Mikrostrukturphysik, Weinberg 2, D-06120 Halle, Germany

(Received 1 April 1998)

The spin dynamics in Ni is studied by an exact diagonalization method on the ultrafast time scale. It is shown that the femtosecond relaxation of the magneto-optical response results from exchange interaction and spin-orbit coupling. Each of the two mechanisms affects the relaxation process differently. We find that the intrinsic spin dynamics occurs during about 10 fs while extrinsic effects such as laser-pulse duration and spectral width can slow down the observed dynamics considerably. Thus, our theory indicates that there is still room to accelerate the spin dynamics in experiments. [S0163-1829(98)51034-X]

The potential application of ferromagnetic materials on ultrafast time scale is attractive for information storage, especially in magneto-optical recording. Both experimentally and theoretically the ultrashort time behavior of spin dynamics in transition metals is a new and challenging area. Vaterlaus *et al.*¹ studied the spin dynamics in ferromagnetic Gd. Employing spin- and time-resolved photoemission with 60-ps probe pulses they found a spin-lattice relaxation (SLR) of 100 ± 80 ps. Using femtosecond optical and magneto-optical pump-probe techniques, Beaurepaire *et al.*² have studied the relaxation processes of electrons and spins in ferromagnetic Ni. They reported that the magnetization of a 22-nm-thick film drops rapidly during the first picosecond and reaches its minimum after 2 ps. Recently, by time-resolved second harmonic generation (SHG), Hohlfeld *et al.*³ found that even when electrons and lattice have not reached a common thermal equilibrium, the classical $M(T)$ curve can be reproduced for delay times longer than the electron thermalization time of about 280 fs. On the other hand, the transient magnetization reaches its minimum ≈ 50 fs before electron thermalization. Both groups used polycrystalline Ni but different pulse durations: 60 fs (Ref. 2) vs 150 fs.³ Recently even faster spin decays have been observed.⁴

A present, not even the mechanism for this ultrafast spin relaxation is known. Moreover, it is of great importance to know whether these results already reflect the intrinsic spin relaxation time scale or not. Theoretically, even the *static* ferromagnetism in transition metals has been a challenging topic as the electron correlation is very strong in these systems.⁵ The theoretical treatment of the spin *dynamics* is limited. On the longer time scales, SLR has been studied previously,⁶ and the theory yielded a relaxation time of 48 ps for Gd, in good agreement with the above-mentioned experiment.¹ On this time scale, the main contributions results from anisotropic phonon-magnon interaction. To our knowledge, so far no theoretical study has been performed about the spin dynamics of transition metals on the *femtosecond* time scale, which is apparently needed.

For the theoretical description of ultrafast nonequilibrium charge and spin dynamics, one can either rely on the Baym-Kadanoff-Keldysh Green's-function approach⁷ or employing an exact diagonalization framework. In this paper, we prefer the later method, which does not involve perturbation theory. Thus it is more suitable to optical excitations away from equilibrium, especially in the presence of strong electron correlations. Our Hamiltonian reads

$$H = \sum_{i,j,k,l,\sigma,\sigma',\sigma'',\sigma'''} U_{i\sigma,j\eta',l\sigma'',k\sigma'''} c_{i\sigma}^\dagger c_{j\sigma'}^\dagger c_{k\sigma''} c_{l\sigma'''} + \sum_{\nu,\sigma,K} \mathcal{E}_\nu(K) n_{\nu\sigma}(K) + H_{SO}, \quad (1)$$

where $U_{i\sigma,j\sigma',l\sigma'',k\sigma''}$ is the on-site electron interaction, which plays an important role in ferromagnetism and can be described in full generality by three parameters: Coulomb repulsion U , exchange interaction J , and exchange anisotropy ΔJ . The generic values for Ni [$U_0 = 12$ eV, $J_0 = 0.99$ eV, and $(\Delta J)_0 = 0.12$ eV] are obtained by fitting the spectroscopic data; for the details see Ref. 8. $c_{i\sigma}^\dagger$ ($c_{i\sigma}$) are the usual creation (annihilation) operators in the orbital i with spin σ ($\sigma = \uparrow \downarrow$). $\mathcal{E}_\nu(K)$ represents the spin-independent band structure of a Ni monolayer. To get it, we need six parameters (for details, see Ref. 9). $n_{\nu\sigma}(K)$ is the particle number operator of band ν in K space. H_{SO} is the spin-orbit coupling.^{10,11} A Hamiltonian of this kind is general enough to address the spin dynamics on the ultrafast time scale as it contains the necessary ingredients. However it is not possible to solve it without approximation.¹² For each K point, the dimension of the two-hole basis for nickel is 66, where six orbitals per spin are taken into account, namely five $3d$ orbitals and one $4s$ orbital. We solve the 66-state problem analytically for each atom. This solution is embedded in the crystal field given by the band structure including the translational variance. This amounts to a crystal field theory, where the embedding is of single electron nature. Thus it can be solved without too much numerical problems. Although we did not

map it to the impurity problem, we believe that our treatment is similar to a K -dependent self-energy correction as performed in the dynamical mean-field theory. Once we construct the Hamiltonian within the above basis, we can diagonalize it directly (for more details see Ref. 8).

Before we go further, it is worth checking whether our Hamiltonian reasonably describes transition metals such as nickel. Once the spin-orbit coupling is switched off, $\{S^2, S_z\}$ are good quantum numbers. First, in the absence of the explicit electron interaction ($U=J=\Delta J=0$), the band structure $\mathcal{E}_p(K)$ is well reproduced with six fitting parameters (given in Ref. 9). Second, the atomic symmetry is well preserved, yielding the correct degeneracies. Third, with non-zero Coulomb interaction U and exchange interaction J , the ground state is ferromagnetic,¹³ which is consistent with the ferromagnetism of the Ni thin film. However, for $U=J=0$, the ground state is a singlet. It is interesting to note that the ferromagnetism exclusively results from the Coulomb and exchange interactions. This is a nontrivial result.

The parameters affecting femtosecond spin dynamics fall in two classes: intrinsic (material specific) and extrinsic (experiment specific). Intrinsic parameters are: (i) Coulomb interaction U , (ii) exchange interaction J , (iii) exchange anisotropy ΔJ , (iv) spin-orbit coupling (SOC) λ , and (v) band structure $\mathcal{E}_p(K)$. Extrinsic parameters include: (vi) the photon frequencies for the pump and probe pulses, (vii) different optical techniques such as pump-probe spectroscopy of reflectivity and magneto-optics, SHG, or two-photon photoemission (TPPE), (viii) flux of the pulse, (ix) laser spectral width, and (x) optical pulse duration. For a given sample, one can vary these external parameters to actively tune the spin dynamics rather than to only passively observe it. In this paper we focus on the effects of (ii), (iv), (v), and (ix).

Experimentally when the system is pumped, the excited-state distribution is formed. We populate the states according to a Gaussian distribution with width W , which mimics the experimental pump pulse. The center of the populated states is around 2 eV above the ground state. The initial excited state will evolve in time with a phase factor according to Schrödinger's equation.

For the charge and spin dynamics, the response functions to the probe pulse are different. It is noted that this response is weak and thus is calculated by linear-response theory. The diagonal element $|\chi_{zz}^{(1)}|$ of the optical susceptibility mainly reflects the contribution from the charge dynamics while $|\chi_{xy}^{(1)}|$ mostly reflects the contribution from the spin dynamics. With the help of those two functions, we are able to address the different characters of the charge and spin dynamics separately. Once the eigenstates are known, $|\chi_{zz}^{(1)}|$ and $|\chi_{xy}^{(1)}|$ are calculated from the usual Lindhard function¹⁰ where the only exception is that the population of the eigenstates is time dependent and complex (with absolute values and phases). The details of it are beyond the scope of the present paper and will be given elsewhere.¹⁴

In the following we monitor both charge and spin dynamics on the fs time scale and investigate the influence of different intrinsic and extrinsic parameters. We start with the generic set of parameters, U_0 , J_0 , and $(\Delta J)_0$ for Ni. The Gaussian width W of the initial excited state is taken as broad as 20 eV in order to maximize the number of available chan-

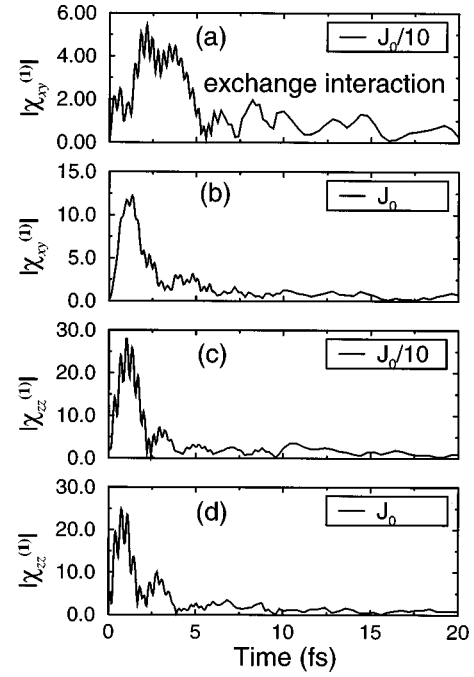


FIG. 1. Effect of exchange interaction J ($J=J_0/10$ and J_0) on spin [(a) and (b)] and charge dynamics [(c) and (d)]. Exchange interaction dominates the spin decay.

nels and thus reveal the intrinsic charge and spin responses. In Figs. 1(b) and 1(d), $|\chi_{xy}^{(1)}(\omega, t)|$ and $|\chi_{zz}^{(1)}(\omega, t)|$ are shown, which represent the spin and charge dynamics, respectively, as measured by typical pump-probe experiments. $\omega=2$ eV hereafter. The relaxation time is determined by looking at the first clear minimum¹⁵ of $|\chi_{xy}^{(1)}(\omega, t)|$ and $|\chi_{zz}^{(1)}(\omega, t)|$. First, the figure shows that charge and spin dynamics occur on a ten-femtosecond time scale,¹⁶ which is much shorter than that in existing experiments. The second important result is that the spin dynamics lags behind the charge dynamics by 1 fs, which is an appreciable effect on a time scale of 3 fs and in accordance with the recent measurement of the spin-dependent lifetime.⁴ This result is very important for possible applications in magnetic storage technology, as it guarantees a nonequilibrium spin memory time. We note in passing that at no stage of our calculation did we have to invoke the notion of either electron or spin temperature. Particularly the concept of spin temperature is questionable not only due to the nonequilibrium, but also due to the absence of well-defined quasiparticle statistics for the spins.

In order to pinpoint the origin of the spin dynamics, we first vary the exchange interaction while the Coulomb interaction $U=U_0$ is fixed. For reduced $J=J_0/10$ [Figs. 1(a) and 1(c)], one can see a more clearly different behavior between spin and charge dynamics. Figures 1(a) and 1(b) show that the exchange interaction affects not only the main peaks of $|\chi_{xy}^{(1)}(\omega, t)|$, but also its subsequent decay: with the decrease of J from J_0 to $J_0/10$, the relaxation time for the spin dynamics increases from 3.4 to 5.6 fs (Ref. 16) while the charge dynamics is virtually unaffected by the variation of J [see Figs. 1(c) and 1(d)]. Thus with decreasing J , the spin dynamics begins later and lags more and more behind the charge dynamics.

Our calculations show that the relaxation time can be

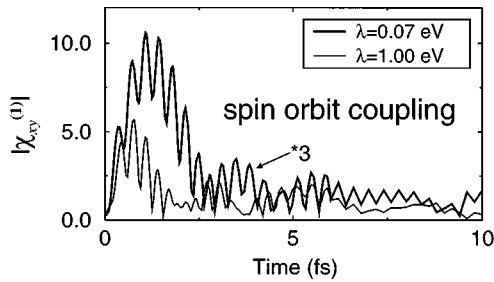


FIG. 2. Effect of spin-orbit coupling λ on spin dynamics. The solid curve is for $\lambda=0.07$ eV while the dashed curve is for $\lambda=1$ eV. SOC may speed up the spin dynamics only in heavy elements.

changed by tuning the exchange strength. Physically ferromagnetism mainly results from the exchange interaction, but it has been unknown how the exchange interaction affects the spin dynamics on the ultrafast time scale. Here we clearly see that it accelerates the relaxation: since in the ferromagnetic system the energy scales roughly as J , the relaxation time scales a $1/J$. Without SOC, the total spin is a good quantum number, yet the spin dynamics exclusively results from the loss of the quantum coherence due to the dephasing of the initial excited state. The information of this dephasing is contained in $|\chi_{xy}^{(1)}(\omega, t)|$ and $|\chi_{zz}^{(1)}(\omega, t)|$, due to the time evolution of the complex population of the eigenstates, and the dephasing occurs on different time scales for charge and spin dynamics.

When the spin-orbit coupling λ is turned on to its generic value $\lambda_0=0.07$ eV, the spin relaxation time is determined by both λ and J . To see the effect of SOC on the relaxation process more clearly, we set $J=\Delta J=0$ and chose $\lambda=0.07, 1.0$ eV. Figure 2 shows that the relaxation time decreases if λ is larger while the main peak of the spectrum becomes narrower. Thus for some noble metals or rare earths with a much larger SOC than that in Ni, optical alignment could generate an ultrafast spin dynamics in TPPE even from non-magnetic metals.¹⁷

Next we study how band structure changes spin and charge dynamics to demonstrate its material sensitivity. We change the band structure multiplying all the hopping integrals by a factor of 0.1. A smaller hopping integral corresponds to a more atomlike material. Figures 3(a) and 3(b) show the spin and charge dynamics, respectively. Comparing Figs. 1(b) and 1(d) with the solid curves in Figs. 3(a) and 3(b), one may note that upon decreasing the hopping integral from A_0 and $A_0/10$, the recurrent features in both $|\chi_{xy}^{(1)}(\omega, t)|$ and $|\chi_{zz}^{(1)}(\omega, t)|$ are more obvious and the relaxation time for the spin dynamics increases up to more than 20 fs for $A_0/10$ (note the different abscissa scales). Thus a small hopping integral as appearing in nanostructured thin films, islands, clusters, or some impurities in the material, slows down the spin dynamics. This means that, e.g., oxides,¹⁸ exhibiting both dispersive bands and nondispersive gap states, might be an ideal playground to tune the dynamical time scale at will. Besides, the reduction of the pulse width from 20 to 0.2 eV further prolongs the decay time to 100 fs [long dashed curves in Figs. 3(a) and 3(b)], which then should be easily accessible by standard experimental techniques. So the laser width (spectral and temporal) has a

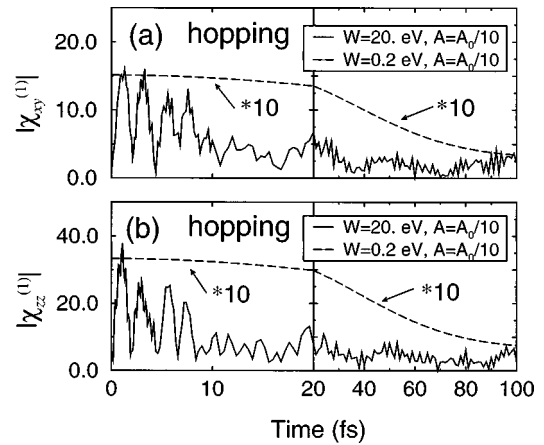


FIG. 3. Effect of hopping integral on (a) spin and (b) charge dynamics. The pulse width effect is also shown. Nanostructuring and selective population of resonances slow down the spin and charge dynamics.

very important impact on the relaxation time of spin dynamics, which deserves a detailed study.

For the investigation of the effect of the laser spectral width (an extrinsic parameter), we choose two different widths of initial state distribution, namely, $W=20$ eV [full curves in Figs. 4(a) and 4(b)] and 0.2 eV (long dashed curves), keeping the other parameters at their generic values $U_0, J_0, (\Delta J)_0, A_0$, and λ_0 . With the decrease of the width, the relaxation time is prolonged greatly. From Fig. 4(a), one may notice that for $W=20$ eV, the decay of the spin dynamics is around 3.4 fs; for $W=0.2$ eV, it prolongs to 14 fs. The pulse-width dependent relaxation is also obvious for the charge dynamics [see Fig. 4(b)]. For $W=20$ eV, it decays around 2 fs; for $W=0.2$ eV, it lasts up to 13 fs. For real applications, the persistence of the slower decay of the spin dynamics compared to the charge dynamics is important as it sets the magnetic memory time. Thus one can change extrinsic parameters to influence the spin dynamics even if one does not change material parameters.

In conclusion, starting from a many-body Hamiltonian, we studied the spin dynamics on the femtosecond scale as a function of intrinsic and extrinsic parameters. Our calculation suggests that the high-speed limit of intrinsic spin dy-

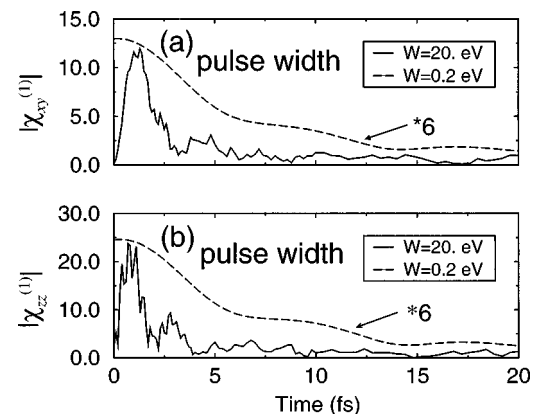


FIG. 4. Effect of laser pulse width W on (a) spin and (b) charge dynamics for $W=20$ and 0.2 eV. Monochromatic laser pulses slow down the dynamics.

namics is about tens of femtoseconds, which is not yet exhausted by experiments. This ultrafast dynamics results from the exchange interaction and SOC and does not involve the lattice.¹⁹ It is very different from SLR in Ref. 1. The SLR time in Ni is about 304 ps as calculated from a formalism similar to that applied to Gd before,⁶ which can be compared with the experimental value of 400 ps in Ni.²⁰ Thus, in total one has to distinguish four different relaxation processes: (a) electronic equilibration (1 fs, due to electron-electron interaction); (b) electron-spin relaxation (a few fs due to exchange interaction or SOC); (c) electron-lattice thermaliza-

tion (≈ 1 ps, due to electron-photon coupling); (d) SLR (≈ 100 ps due to SOC plus anisotropic crystal-field fluctuations).

One of us (W.H.) gratefully acknowledges the hospitality of the IPCMS of Strasbourg, where a major part of this work has been performed, and stimulating discussions with E. Beaurepaire, J.-Y. Bigot, D. C. Langreth, J.-C. Merle, and P. Nordlander. This work has been supported by IPCMS Strasbourg and the TMR on NOMOKE (ERB-FMRX-CT 96-0015).

*Electronic address: zhang@volley.mpi-halle.mpg.de

¹A. Vaterlaus, T. Beutler, and F. Meier, Phys. Rev. Lett. **67**, 3314 (1991).

²E. Beaurepaire, J.-R. Merle, A. Daunois, and J. Y. Bigot, Phys. Rev. Lett. **76**, 4250 (1996).

³J. Hohlfeld, E. Matthias, R. Knorren, and K. H. Bennemann, Phys. Rev. Lett. **78**, 4861 (1997); **79**, 960(E) (1997).

⁴M. Aeschlimann, M. Bauer, S. Pawlik, W. Weber, R. Burgermeister, D. Oberli, and H. C. Siegmann, Phys. Rev. Lett. **79**, 5158 (1997).

⁵P. Fulde, *Electron Correlation in Molecules and Solids*, 3rd ed. (Springer, Heidelberg, 1995); J. Wahle, N. Blümer, J. Schling, K. Held, and D. Vollhardt, cond-mat/9711242 (unpublished).

⁶W. Hübner and K. H. Bennemann, Phys. Rev. B **53**, 3422 (1996).

⁷H. Shao, P. Nordlander, and D. C. Langreth, Phys. Rev. Lett. **77**, 948 (1966).

⁸W. Hübner and L. M. Falicov, Phys. Rev. B **47**, 8783 (1993); C. Moore, *Atomic Energy Levels*, Natl. Bur. Stand. (U.S.) (U.S. GPO, Washington, DC, 1971).

⁹W. Hübner, Phys. Rev. B **42**, 11 553 (1990); A. Lessard, T. H. Moos, and W. Hübner, *ibid.* **56**, 2594 (1997); T. H. Moos, W. Hübner, and K. H. Bennemann, Solid State Commun. **98**, 639 (1996).

¹⁰Normally, Fermi-liquid theory only treats spin-spin interaction neglecting the orbital contribution to the electronic interaction. For thin films this might be a major deficiency. G. D. Mahan, *Many-Particle Physics*, 2nd ed. (Plenum, New York, 1990), p. 899.

¹¹H. Takayama, K. Bohnen, and P. Fulde, Phys. Rev. B **14**, 2287 (1976).

¹²Methods going beyond the present approximation may become

rather impractical, especially when one is mainly interested in the excited states rather than only the ground state. For example, for 1000 K points as typically used in our calculations, the dimension of the total Hilbert space would exceed 10^{1000} , which is intractable for the present computational facilities.

¹³A ferromagnetic state is defined to be a state with multiplicities other than singlets or Kramers doublets.

¹⁴W. Hübner and G. P. Zhang (unpublished).

¹⁵Obviously there is no clear exponential envelope visible on this fast time scale. Thus our definition seems to be an appropriate choice.

¹⁶The relaxation time refers to the *delay time* between the probe and pump pulses, which can be detected experimentally. It can be as short as attoseconds as experiments revealed recently [see H. Petek, A. P. Heberle, W. Nessler, H. Nagano, S. Kubota, S. Matsunami, N. Moriya, and S. Ogawa, Phys. Rev. Lett. **79**, 4649 (1997); M. U. Wehner, M. H. Ulm, D. S. Chemla, and M. Wegener, *ibid.* **80**, 1992 (1998)]. The process occurs in the real time domain and the average over “one period of the light” is not needed.

¹⁷N. I. Zheludev, P. J. Bennett, H. Loh, S. V. Popov, I. R. Shatwell, Y. P. Svirko, V. E. Gusev, V. F. Kamalov, and E. V. Slobodchikov, Opt. Lett. **20**, 1368 (1995).

¹⁸P. Kner, S. Bar-Ad, M. V. Marquezini, D. S. Chemla, and W. Schäfer, Phys. Rev. Lett. **78**, 1319 (1997).

¹⁹The slow recovery of the spin resonance during several hundred picoseconds seen in experiments results from the lattice and is beyond the scope of the present study.

²⁰A. Scholl, L. Baumgarten, and W. Eberhardt, Phys. Rev. Lett. **79**, 5146 (1997).